product. However, in the Pd(II) series the thermal barrier leading to the formation of the trans product must lie near or below the energy level of the typical complex formation reaction conditions, since the trans isomer is the one usually observed.

The inclusion of the phosphorus extrusion process into the series of organometallic preparative reactions will provide a novel alternative to those presently available.[22] Considering the number of phosphines commercially available, this method of preparation should lead to the synthesis of many new complexes heretofore unaccessible by standard routes.

(22) Wilkinson, G., Stone, F. G. A., Abel, E. W., Eds. *Comprehensive Organometallic Chemistry: The Synthesis, Reactions and Structures of Organometallic Compounds*; Pergamon: Oxford, New York, 1982; Vol. 2-6.

Acknowledgment. We wish to thank the National Science Foundation and the Center for Energy Studies, Louisiana State University, for partial support of this work.

Registry No. **1**, 68469-71-6; **2**, 110173-82-5; **2**·C_6H_6, 110173-84-7; **3**, 110173-83-6; **3**·C_6H_6, 110173-85-8; **4**, 14871-92-2; **5**, 110222-28-1; **6**, 110144-23-5; **7**, 110191-20-3; **8**, 87039-36-9; $PdCl_2$, 7647-10-1; $(Ph_2P)_2$-2,6-pyr, 64741-27-1; Na_2PdCl_4, 13820-53-6.

Supplementary Material Available: Listings of bond distances and angles (Tables S1, S4, S7, and S10), calculated hydrogen coordinates and refined isotropic thermal parameters (Tables S2, S5, S8, and S11), and anisotropic thermal parameters (Tables S3, S6, S9, and S12) for complexes **2**, **2**·C_6H_6, **3**·C_6H_6, and **7** and additional atomic coordinates and thermal parameters for **7** (Table S17) (40 pages); listings of observed and calculated structure factors (Tables S13-S16) (98 pages). Ordering information is given on any current masthead page.

Contribution from the Department of Chemistry, University of Minnesota, Minneapolis, Minnesota 55455

Heterobimetallic Au-Ir, Ag-Ir, and Au-Ru Bis(μ-hydrido) Complexes. X-ray Crystal and Molecular Structures of $[AuRu(H)_2(dppm)_2(PPh_3)]PF_6$ and $[Ir(H)_2(bpy)(PPh_3)_2]PF_6$

Bruce D. Alexander, Brian J. Johnson, Steven M. Johnson, Paul D. Boyle, Nina C. Kann, Ann M. Mueting, and Louis H. Pignolet*

Received April 1, 1987

Several new heterobimetallic hydrides containing Au or Ag have been synthesized. $[AuRu(H)_2(dppm)_2(PPh_3)]PF_6$ (**3**) was made by the reaction of $AuPPh_3NO_3$ with $Ru(H)_2(dppm)_2$ with the use of acetone as solvent. $[AgIr(H)_2(bpy)(PPh_3)_2](O_3SCF_3)(BF_4)$ (**5**), $[AgIr(H)_2(bpy)(PPh_3)_2(NO_3)](BF_4)$ (**6**), and $[AuIr(H)_2(bpy)(PPh_3)_2(CH_3CN)](BF_4)_2$ (**7**) were synthesized by the reaction of the BF_4^- salt of $[Ir(H)_2(bpy)(PPh_3)_2](PF_6)$ (**4**) with AgO_3SCF_3, $AgNO_3$, and $Au(CH_3CN)_2BF_4$, respectively, and $[AgIr(H)_2(bpy)(PPh_3)_3](O_3SCF_3)(BF_4)$ (**8**) was made by the reaction of PPh_3 with **5**. Compounds **3** and **4** were characterized by single-crystal X-ray diffraction in the solid state (**3**, $P2_1/n$, a = 19.456 (7) Å, b = 15.049 (5) Å, c = 23.843 (4) Å, β = 113.41 (3)°, T = -91 °C, R = 0.050; **4**, $P2_1/c$, a = 11.677 (3) Å, b = 21.723 (7) Å, c = 17.680 (1) Å, β = 92.70 (4)°, T = -85 °C, R = 0.041) and by ^{31}P and ^1H NMR spectroscopy in solution. In both complexes the hydride ligands were directly observed by X-ray diffraction and in **3** were found to bridge the Ru-Au bond. The average Ru-H and Au-H distances in **3** are 1.71 (6) and 1.98 (6) Å, respectively, and the Ru-Au separation is 2.694 (1) Å. The average Ir-H and Ir-N distances in **4** are 1.51 (6) and 2.150 (5) Å, respectively. Comparison of the Ir-N distances in **4** and those of the previously characterized $AuPPh_3$ adduct of **4** $[AuIr(H)_2(bpy)(PPh_3)_3](BF_4)_2$ (**2**) provides further support for a bridging dihydride formulation of the latter. Compounds **5-8** were also determined to have bridging hydrides by NMR and IR spectroscopy.

Introduction

There has been considerable interest recently in the synthesis and structural characterization of mixed transition-group 1B (11^{64}) clusters.[1-31] These compounds are important because of their intrinsically novel structures and properties, their potential use as bimetallic catalysts, and their potential to aid in under-

(1) Boyle, P. D.; Johnson, B. J.; Alexander, B. D.; Casalnuovo, J. A.; Gannon, P. R.; Johnson, S. M.; Larka, E. A.; Mueting, A. M.; Pignolet, L. H. *Inorg. Chem.* **1987**, *26*, 1346.
(2) Alexander, B. A.; Johnson, B. J.; Johnson, S. M.; Casalnuovo, A. L.; Pignolet, L. H. *J. Am. Chem. Soc.* **1986**, *108*, 4409 and references cited therein.
(3) Boyle, P. D.; Johnson, B. J.; Buehler, A.; Pignolet, L. H. *Inorg. Chem.* **1986**, *25*, 5.
(4) Casalnuovo, A. L.; Casalnuovo, J. A.; Nilsson, P. V.; Pignolet, L. H. *Inorg. Chem.* **1985**, *24*, 2554.
(5) Casalnuovo, A. L.; Laska, T.; Nilsson, P. V.; Olofson, J.; Pignolet, L. H.; Bos, W.; Bour, J. J.; Steggerda, J. J. *Inorg. Chem.* **1985**, *24*, 182.
(6) Casalnuovo, A. L.; Pignolet, L. H.; van der Velden, J. W. A.; Bour, J. J.; Steggerda, J. J. *J. Am. Chem. Soc.* **1983**, *105*, 5957.
(7) Bos, W.; Bour, J. J.; Schlebos, P. P. J.; Hageman, P.; Bosman, W. P.; Smits, J. M. M.; van Wietmarschen, J. A. C.; Beurskens, P. T. *Inorg. Chim. Acta* **1986**, *119*, 141.
(8) Mingos, D. M. P.; Wardle, R. W. M. *J. Chem. Soc., Dalton Trans.* **1986**, 73. Gilmour, D. I.; Mingos, D. M. P. *J. Organomet. Chem.* **1986**, *302*, 127 and references cited therein.
(9) Briant, C. E.; Gilmour, D. I.; Mingos, D. M. P. *J. Chem. Soc., Dalton Trans.* **1986**, 835.
(10) Hall, K. P.; Mingos, D. M. P. *Prog. Inorg. Chem.* **1984**, *32*, 237.
(11) Teo, B. K.; Keating, K. *J. Am. Chem. Soc.* **1984**, *106*, 2224. See also: *Chem. Eng. News* **1987**, *65*(2), 21.
(12) Henly, T. J.; Shapley, J. R.; Rheingold, A. L. *J. Organomet. Chem.* **1986**, *310*, 55.
(13) Lauher, J. W.; Wald, K. *J. Am. Chem. Soc.* **1981**, *103*, 7648.
(14) Braunstein, P.; Lehner, H.; Matt, D.; Tiripicchio, A.; Tiripicchio-Camellini, M. *Angew. Chem., Int. Ed. Engl.* **1984**, *23*, 304 and references cited therein.
(15) Johnson, B. F. G.; Lewis, J.; Nelson, W. J. H.; Raithby, P. R.; Vargas, M. D. *J. Chem. Soc., Chem. Commun.* **1983**, 608.
(16) Farrugia, L. J.; Freeman, M. J.; Green, M.; Orpen, A. G.; Stone, F. G. A.; Salter, I. D. *J. Organomet. Chem.* **1983**, *249*, 273.
(17) Braunstein, P.; Rose, J.; Manotti-Lanfredi, A. M.; Tiripicchio, A.; Sappa, E. *J. Chem. Soc., Dalton Trans.* **1984**, 1843.
(18) Hutton, A. T.; Pringle, P. O. G.; Shaw, B. L. *Organometallics* **1983**, *2*, 1889.
(19) Braunstein, P.; Carneiro, T. M. G.; Matt, D.; Tiripicchio, A.; Camellini, M. T. *Angew. Chem., Int. Ed. Engl.* **1986**, *25*, 748.
(20) Freeman, M. J.; Green, M.; Orpen, A. G.; Salter, I.; Stone, F. G. A. *J. Chem. Soc., Chem. Commun.* **1983**, 1332.
(21) Connelly, N. G.; Howard, J. A. K.; Spencer, J. L.; Woodley, P. K. *J. Chem. Soc., Dalton Trans.* **1984**, 2003.
(22) Bates, P. A.; Brown, S. S. D.; Dent, A. J.; Hursthouse, M. B.; Kitchen, F. G. M.; Orpen, A. G.; Salter, I. D.; Sik, V. *J. Chem. Soc., Chem. Commun.* **1986**, 600.
(23) Bachechi, F.; Ott, J.; Venanzi, L. M. *J. Am. Chem. Soc.* **1985**, *107*, 1760. Albinati, A.; Dahmen, K. H.; Togni, A.; Venanzi, L. M. *Angew. Chem., Int. Ed. Engl.* **1985**, *24*, 766.
(24) Easton, T.; Gould, R. O.; Heath, G. A.; Stephenson, T. A. *J. Chem. Soc., Chem. Commun.* **1985**, 1741.

0020-1669/87/1326-3506$01.50/0 © 1987 American Chemical Society

standing the role of gold and silver in supported alloy catalysts.[32-34] Most complexes in this category involve clusters that contain transition metals with one or more $AuPR_3$ units. These compounds often illustrate a close similarity between a metal hydride ligand and a $AuPPh_3$ unit, the so-called isolobal analogy.[12,13,35]

In comparison to the case for the gold systems, there are fewer structurally characterized examples of mixed transition-metal–silver clusters that contain primarily phosphine ligands.[11,19-27] Widely applicable synthetic routes to such compounds are not available, and characterization of such compounds is often difficult. This is in part due to silver's redox chemistry[36] and the lability of ligands bound to silver.

Recently, we reported the synthesis, single-crystal X-ray analysis, and spectroscopic characterization of two transition-metal–gold hydride clusters, $[Au_2Ru(H)_2(dppm)_2(PPh_3)_2](NO_3)_2$ (**1**; dppm = bis(diphenylphosphino)methane) and $[AuIr(H)_2(bpy)(PPh_3)_3](BF_4)_2$ (**2**; bpy = 2,2′-bipyridine).[2] In **1** the hydride

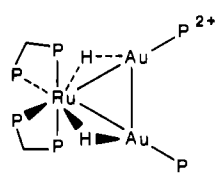

cation of **1**

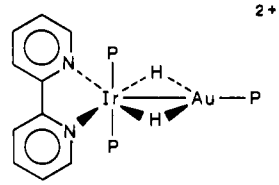

cation of **2**

ligands were located and refined in the X-ray analysis and were found to be bridging between the Au and Ru atoms as shown in the drawing. In **2** the hydrides were not located in the X-ray analysis, but evidence was provided that strongly supported a bridging mode in this complex also.[2] Since the structures and reactivity of these and other transition-metal–gold hydride clusters[3-6] are important in understanding gold and gold alloy surface catalysis,[32,34] and since gold–hydride interactions are likely in gold-surface-catalyzed H_2/D_2 exchange and olefin hydrogenation reactions,[34] it is especially important to fully elucidate the bonding modes of the hydride ligands. Therefore, additional studies were performed on related ruthenium- and iridium–gold compounds in order to obtain further information concerning gold–hydride interactions. The iridium chemistry was also expanded to include the study of iridium–silver complexes in an effort to explore the analogous cluster chemistry of silver.

In this paper we report the synthesis, single-crystal X-ray analysis, and spectroscopic characterization of a new ruthenium–gold compound, $[AuRu(H)_2(dppm)_2(PPh_3)]PF_6$ (**3**), and the single-crystal X-ray analysis of $[Ir(H)_2(bpy)(PPh_3)_2]PF_6$ (**4**). In both **3** and **4** the hydride ligands were located and refined in the X-ray analysis, and in **3** the hydrides were found to be bridging between the Au and Ru atoms. Analysis of the structure of **4** and comparison to that of **2** provided further support for the dihydride bridging mode in **2**. We also report here the synthesis, characterization, and chemistry of some new transition-metal–group 1B hydride clusters prepared from the BF_4^- salt of **4**. The new compounds are $[AgIr(H)_2(bpy)(PPh_3)_2](O_3SCF_3)(BF_4)$ (**5**), $[AgIr(H)_2(bpy)(PPh_3)_2(NO_3)](BF_4)$ (**6**), $[AuIr(H)_2(bpy)(PPh_3)_2(CH_3CN)](BF_4)_2$ (**7**), and $[AgIr(H)_2(bpy)(PPh_3)_3](O_3SCF_3)(BF_4)$ (**8**). These complexes do not contain phosphines bound to the coinage metal but have weakly held ligands associated with them.

Experimental Section

Physical Measurements and Reagents. ^1H and ^{31}P NMR spectra were recorded at 300 and 121.5 MHz, respectively, with the use of a Nicolet NT-300 spectrometer. ^{31}P NMR spectra were run with proton decoupling and are reported in parts per million (ppm) relative to the internal standard trimethyl phosphate (TMP) with positive shifts downfield. Infrared spectra were recorded on a Beckman Model 4250 grating spectrometer. Conductivity measurements were made with the use of a Yellow Springs Model 31 conductivity bridge. Compound concentrations used in the conductivity experiments were 3×10^{-4} M in CH_3CN or CH_3NO_2. Microanalyses were carried out by M-H-W Laboratories, Phoenix, AZ. Solvents were dried and distilled prior to use. $AuPPh_3NO_3$,[37] $Ru(H)_2(dppm)_2$,[38] and $[Ir(H)_2(bpy)(PPh_3)_2]BF_4$[2] were prepared as described in the literature. $Au(CH_3CN)_2BF_4$ was prepared by analogy to the literature procedure[39] for the ClO_4^- salt using $NOBF_4$. Bis(diphenylphosphino)methane, dppm, was purchased from Strem Chemicals, Inc., silver triflate, AgO_3SCF_3, and $RuCl_3 \cdot 3H_2O$ were purchased from Aldrich, and 2,2′-bipyridine, bpy, was purchased from Eastman Organic Chemicals. All manipulations were carried out under a purified N_2 atmosphere with use of standard Schlenk techniques unless otherwise noted.

Preparation of Compounds. **$[AuRu(H)_2(dppm)_2(PPh_3)]PF_6$ (3)** was prepared by reacting $Ru(H)_2(dppm)_2$ (142 mg, 0.163 mmol) with $AuPPh_3NO_3$ (85.4 mg, 0.163 mmol) in 5 mL of acetone. The resulting light yellow solution was stirred at ambient temperature for 1 h, during which time a white microcrystalline product began to precipitate. Complete precipitation occurred upon the addition of 15 mL of Et_2O. The solid was then collected, redissolved in CH_2Cl_2, and filtered into a MeOH solution that contained 200 mg of KPF_6. A white precipitate formed and was collected, washed with cold MeOH and Et_2O, and dried in vacuo. The yield was 199 mg (83%). Recrystallization from a CH_2Cl_2–Et_2O solvent mixture at ambient temperature produced pale yellow rectangular crystals suitable for X-ray diffraction. $^{31}P\{^1H\}$ NMR (acetone, 25 °C): δ 45.67 (t, J = 23.8 Hz, int = 1), 3.72 (t of d, J = 36.9 and 23.8 Hz, int = 2), −0.26 (t, J = 36.9 Hz, int = 2). ^1H NMR in hydride region (acetone-d_6, 25 °C): δ −4.4 (d of d of t, J_{H-P_A} = 54.0 Hz, J_{H-P_B} = 32.3 Hz, J_{H-P_C} = 12.4 Hz). The equivalent conductance (85.7 cm^2 mho mol^{-1}) is indicative of a 1:1 electrolyte in CH_3CN solution. Anal. Calcd for $AuRuP_6C_{68}H_{61}F_6$: C, 55.3; H, 4.17; P, 12.59. Found: C, 54.84; H, 4.18; P, 12.72.

$[Ir(H)_2(bpy)(PPh_3)_2]PF_6$ (4) was prepared by the addition of excess NH_4PF_6 (270 mg, 4.7 mmol) in 5 mL of MeOH to a CH_2Cl_2 solution of $[Ir(H)_2(bpy)(PPh_3)_2]BF_4$[2] (107 mg, 0.111 mmol). After the mixture was stirred for 30 min, the volume of solvent was reduced and a yellow precipitate formed. About 10 mL of diethyl ether was added to further the precipitation of the pale yellow solid, which was collected on a frit and washed with Et_2O. The solid was redissolved in a small amount of CH_2Cl_2, allowed to pass through the frit, and reprecipitated with diethyl ether. The yellow microcrystalline solid was then collected, washed, and dried under a N_2 stream. The yield was 91 mg (80%). X-ray-quality crystals could be grown by slow CH_2Cl_2–Et_2O diffusion. This compound had spectroscopic properties identical with those of $[Ir(H)_2(bpy)(PPh_3)_2]BF_4$.[2]

$[AgIr(H)_2(bpy)(PPh_3)_2](O_3SCF_3)(BF_4)$ (5). $[Ir(H)_2(bpy)(PPh_3)_2]BF_4$, (380 mg, 0.39 mmol) was dissolved in 10 mL of CH_2Cl_2 and cooled to −78 °C. AgO_3SCF_3 (140 mg, 0.54 mmol) was dissolved in 15 mL of CH_3OH, cooled to −78 °C, and added to the cold solution of the BF_4^- salt of **4**. Upon this addition, the solution color gradually changed from yellow to very pale yellow. The flask was wrapped in aluminum foil and the solution stirred while it was warmed to ca. −10 °C over a period of 2 h. At this point the solution volume was reduced under vacuum and sufficient diethyl ether was added to precipitate a fine white powder. This material was collected on a cooled frit, washed with ether, and dried

(25) Schiavo, S. L.; Bruno, G.; Piraino, P.; Faraone, F. *Organometallics* **1986**, *5*, 1400. Bruno, G.; Schiavo, S. L.; Piraino, P.; Faraone, F. *Organometallics* **1985**, *4*, 1098.
(26) Ladd, J. A.; Hope, H.; Balch, A. L. *Organometallics* **1984**, *3*, 1838.
(27) Bruce, M. I.; Williams, M. L.; Patrick, J. M.; Skelton, B. W.; White, A. H. *J. Chem. Soc., Dalton Trans.* **1986**, 2557.
(28) Green, M.; Orpen, A. G.; Salter, I. D.; Stone, F. G. A. *J. Chem. Soc., Dalton Trans.* **1984**, 2497.
(29) Rhodes, L. F.; Huffman, J. C.; Caulton, K. G. *J. Am. Chem. Soc.* **1984**, *106*, 6874.
(30) Smith, D. E.; Welch, A. J.; Treurnicht, I.; Puddephatt, R. J. *Inorg. Chem.* **1986**, *25*, 4616.
(31) Edelmann, F.; Töfke, S.; Behrens, U. *J. Organomet. Chem.* **1986**, *309*, 87.
(32) Sinfelt, J. H. *Bimetallic Catalysts*; Wiley: New York, 1983; Chapters 1 and 2.
(33) Evans, J.; Jingxing, G. *J. Chem. Soc., Chem. Commun.* **1985**, 39.
(34) ACS Symposium on Catalysis of the Group 1B Metals, Presented at the 189th National Meeting of the American Chemical Society, Miami Beach, FL, May 1–2, 1985. Schwank, J. *Gold Bull.* **1983**, *16*, 103. Wachs, I. E. *Gold Bull.* **1983**, *16*, 98.
(35) Evans, D. G.; Mingos, D. M. P. *J. Organomet. Chem.* **1982**, *232*, 171.
(36) Blagg, A.; Hutton, A. T.; Shaw, B. L.; Thornton-Pett, M. *Inorg. Chim. Acta* **1985**, *100*, L33.
(37) Malatesta, J.; Naldini, L.; Simonetta, G.; Cariati, F. *Coord. Chem. Rev.* **1966**, *1*, 255.
(38) Chaudret, B.; Commenges, G.; Poilblanc, R. *J. Chem. Soc., Dalton Trans.* **1984**, 1635.
(39) Bergerhoff, V. G. *Z. Anorg. Allg. Chem.* **1964**, *327*, 139.

in vacuo. Three 10-mL portions of CH_2Cl_2 were added to the frit and allowed to pass through, leaving behind the excess insoluble AgO_3SCF_3. Et_2O was added to the flask containing the combined CH_2Cl_2 extracts to precipitate a white or very pale yellow product. After the solid was collected on a frit, washed with Et_2O, and dried in vacuo, 310 mg of **5** was isolated (65% yield). $^{31}P\{^1H\}$ NMR (CH_2Cl_2, −15 °C, 2×10^{-3} M solution): δ 5.1 (s) (the resonance was at δ 4.8 in 1×10^{-3} M solution). ^1H NMR in hydride region (CD_2Cl_2, −15 °C, 1.5×10^{-3} M solution): δ −16.9 (t, J_{P-H} = 12.8 Hz). IR (Kel-F mull): ν(CF_3SO_3 ionic) 1280 cm^{-1}. Conductance (CH_3NO_2, 3×10^{-4} M solution): 105 cm^2 mho mol^{-1} (1:2 electrolyte). Anal. Calcd for $AgIrP_2BC_{47}H_{40}F_7N_2O_3S$: C, 46.32; H, 3.31; N, 2.30. Found: C, 45.74; H, 3.51; N, 2.50.

$[AgIr(H)_2(bpy)(PPh_3)_2(NO_3)](BF_4)$ (6) was synthesized by using the procedure for the synthesis of **5** with 100 mg (0.104 mmol) of $[Ir(H)_2(bpy)(PPh_3)_2]BF_4$ and 30 mg (0.176 mmol) of $AgNO_3$. The product was isolated as a white solid in 76% yield. $^{31}P\{^1H\}$ NMR (CD_2Cl_2, −15 °C): δ 5.9 (s). ^1H NMR in hydride region (CD_2Cl_2, 20 °C): δ −17.3 (t, J_{P-H} = 13.4 Hz). IR (Nujol mull): ν(bpy CN) 1605 cm^{-1}; ν(NO_3 (bound)) 1490, 1480, 1268 cm^{-1}; ν(BF_4) 1040 cm^{-1}. Conductance (CH_3NO_2, 3×10^{-4} M): 72.3 cm^2 mho mol^{-1} (1:1 electrolyte). Anal. Calcd for $AgIrC_{46}H_{40}BF_4N_3O_3P_2$: C, 48.80; H, 3.56; N, 3.71; P, 5.47. Found: C, 48.82; H, 3.71; N, 3.80; P, 5.28.

$[AuIr(H)_2(bpy)(PPh_3)_2(CH_3CN)](BF_4)_2$ (7). The BF_4^- salt of complex **4** (50 mg, 0.104 mmol) was dissolved in 5 mL of CH_2Cl_2 and 6 mL of freshly distilled CH_3CN. The flask containing this solution was cooled to 0 °C and wrapped in aluminum foil. $Au(CH_3CN)_2BF_4$ (80 mg, 0.22 mmol) was dissolved in ca. 5 mL of CH_3CN and transferred via glass pipet to the foil-wrapped flask. Upon addition the solution gradually changed from yellow to colorless, attaining the latter just as the last portion of $Au(CH_3CN)_2^+$ was added. The solution was stirred for 10 min, and diethyl ether was added to precipitate a white product. This material was collected on a cooled frit, washed with ether, and dried with a stream of nitrogen. CH_2Cl_2 was added in three portions to dissolve the product, and the extracts were passed through the frit into a cooled, foil-wrapped flask. Ether was added to precipitate 90 mg of the white product (69% yield). $^{31}P\{^1H\}$ NMR (CH_2Cl_2, −15 °C): δ 2.3 (s). ^1H NMR (CD_2Cl_2, −15 °C): δ 2.07 (s, CH_3CN), −15.6 (t, J_{P-H} = 10.4 Hz). IR (Nujol mull): ν(acetonitrile CN) 2331, 2304 cm^{-1} (w); ν(bpy CN) 1606 cm^{-1} (m); ν(BF_4) 1040 cm^{-1}.

$[AgIr(H)_2(bpy)(PPh_3)_3](O_3SCF_3)(BF_4)$ (8). To a solution of **5** (103 mg, 0.085 mmol) in CH_2Cl_2 at −30 °C was added a solution of PPh_3 (22 mg, 0.084 mmol) in CH_2Cl_2. The solution turned from a very pale yellow to a slightly more intense yellow and was warmed to 0 °C. Et_2O was added to precipitate the off-white product, which was collected on a frit, washed with Et_2O, and dried in vacuo. The yield was 103 mg (82%). $^{31}P\{^1H\}$ (CH_2Cl_2, −80 °C): δ 18.0 (2 d, $AgPPh_3$, $J_{^{109}Ag-P}$ = 708 Hz, $J_{^{107}Ag-P}$ = 613 Hz, int = 1), 3.7 (s, $IrPPh_3$, int = 2). ^1H NMR (CD_2Cl_2, −80 °C): δ −16.3 (apparent d of q of d, J = 51.5, 12.6, 3.1 Hz) (see Results and Discussion). Conductance (CH_3NO_2, 3×10^{-4} M): 112 cm^2 mho mol^{-1} (indicative of 1:2 electrolyte in CH_3NO_2). Anal. Calcd for $AgIrP_3BC_{65}F_7H_{55}N_2O_3S$: C, 52.71; H, 3.74; N, 1.89; P, 6.27. Found: C, 52.57; H, 3.93; N, 1.93; P, 5.28.

X-ray Structure Determination. Collection and Reduction of X-ray Data. A summary of crystal and intensity data for **3** and **4** is presented in Table I. Crystals of both compounds were coated with a viscous high-molecular-weight hydrocarbon and secured to the end of glass fibers by cooling to −91 °C in the case of **3** and −85 °C for **4**. The crystals remained stable at this temperature during data collection. The crystal classes and space groups were unambiguously determined by the Enraf-Nonius CAD4-SDP-PLUS peak search, centering, and indexing programs,[40] by the presence of systematic absences observed during data collection, and by successful solution and refinement (vide infra). The intensities of three standard reflections were measured every 1.5 h of X-ray exposure time, and no decay was observed for either compound. Empirical absorption corrections were applied for both compounds by use of ψ-scan data and the programs PSI and EAC.[40]

Solution and Refinement of the Structures. The structures were solved by conventional heavy-atom techniques. The metal atoms were located by Patterson syntheses, and full-matrix least-squares refinement and difference Fourier calculations were used to locate all remaining non-hydrogen atoms. The atomic scattering factors were taken from the usual tabulation,[41] and the effects of anomalous dispersion were included in F_c by using Cromer and Ibers' values of $\Delta f'$ and $\Delta f''$.[42] Hydrogen atom positions were calculated for all PPh_3, dppm, and bpy ligands and were included in the structure factor calculations but were not refined. All non-hydrogen atoms in both **3** and **4** were refined with anisotropic thermal parameters. The two hydride ligands in both **3** and **4** appeared as the largest peaks in difference Fourier maps on the basis of the totally converged non-hydride-containing structures. In **3**, the temperature factor for one of the hydride ligands, H1, was not well-behaved during refinement. This parameter (B_{iso}) was reset and constrained to have the same value as the other hydride, H2. The hydrides in **3** and **4** were refined and converged with isotropic thermal parameters to give reasonable distances and angles. The largest peaks in the final difference Fourier map of **3** were ca. 1.3 e $Å^{-3}$ and of **4** were ca. 0.9 e $Å^{-3}$ (approximate height of a hydrogen atom) and were located near the PF_6^-

Table I. Summary of Crystal Data and Intensity Collection for **3** and **4**

	$[AuRu(H)_2(dppm)_2(PPh_3)]PF_6 \cdot CH_2Cl_2$ (**3**·CH_2Cl_2)	$[Ir(H)_2(bpy)(PPh_3)_2]PF_6 \cdot CH_2Cl_2$ (**4**·CH_2Cl_2)
Crystal Parameters and Measurement of Intensity Data		
cryst syst	monoclinic	monoclinic
space group	$P2_1/n$ (No. 14)	$P2_1/c$ (No. 14)
cryst dimens, mm^3	0.15 × 0.25 × 0.35	0.4 × 0.35 × 0.2
cell params T, °C	−91	−85
a, Å	19.456 (7)	11.677 (3)
b, Å	15.049 (5)	21.723 (7)
c, Å	23.843 (4)	17.680 (1)
β, deg	113.41 (3)	92.70 (4)
V, $Å^3$	6407 (7)	4480 (5)
Z	4	4
calcd density, g cm^{-3}	1.618	1.638
abs coeff, cm^{-1}	28.0	32.5
max, min, av transmission factors	1.00, 0.76, 0.89	1.00, 0.79, 0.92
formula	$C_{69}H_{63}Cl_2F_6P_6AuRu$	$C_{47}H_{42}Cl_2F_6N_2P_3Ir$
fw	1561.05	1104.89
diffractometer	CAD 4	
radiation	Mo Kα (λ = 0.71069 Å) graphite monochromatized	same as for **3**
scan type; range (2θ), deg	ω scan; 0–50	ω scan; 0–54
unique rflns measd (region)	11 739 (±h,+k,+l)	10035 (+h,+k,±l)
obsd rflns[a]	7585 ($F_o^2 \geq \sigma(F_o^2)$)	6566 ($F_o^2 \geq \sigma(F_o^2)$)
Refinement by Full-Matrix Least Squares		
no. of params	775	559
R[b]	0.050	0.041
R_w[b]	0.053	0.042
GOF[b]	1.43	1.14
p[a]	0.04	0.04

[a] The intensity data were processed as described in: *CAD 4 and SDP-PLUS User's Manual*; B.A. Frenz & Associates: College Station, TX, 1982. The net intensity $I = [K/\text{NPI}](C - 2B)$, where K = 20.1166 (attenuator factor), NPI = ratio of fastest possible scan rate for the measurement, C = total count, and B = total background count. The standard deviation in the net intensity is given by $[\sigma(I)]^2 = (K/\text{NPI})^2[C + 4B + (pI)^2]$ where p is a factor used to downweight intense reflections. The observed structure factor amplitude F_o is given by $F_o = (I/Lp)^{1/2}$, where Lp = Lorentz and polarization factors. The $\sigma(I)$'s were converted to the estimated errors in the relative structure factors $\sigma(F_o)$ by $\sigma(F_o) = {}^1/_2[\sigma(I)/I]F_o$. [b] The function minimized was $\sum w(|F_o| - |F_c|)^2$, where $w = 1/[\sigma(F_o)]^2$. The unweighted and weighted residuals are defined as $R = \sum(||F_o| - |F_c||)/\sum|F_o|$ and $R_w = [(\sum w(|F_o| - |F_c|^2)/(\sum w|F_o|^2)]^{1/2}$. The error in an observation of unit weight (GOF) is $[\sum w(|F_o| - |F_c|)^2/(\text{NO} - \text{NV})]^{1/2}$, where NO and NV are the numbers of observations and variables, respectively.

(40) All calculations were carried out on PDP 8A and 11/34 computers with the use of the Enraf-Nonius CAD 4-SDP-PLUS programs. This crystallographic computing package is described by: Frenz, B. A. In *Computing in Crystallography*; Schenk, H., Olthof-Hazekamp, R., van Konigsveld, H., Bassi, G. C., Eds.; Delft University Press: Delft, Holland, 1978; pp 64–71. Frenz, B. A. In *Structure Determination Package and SDP-PLUS User's Guide*; B. A. Frenz & Associates: College Station, TX, 1982.

(41) Cromer, D. T.; Waber, J. T. *International Tables for X-ray Crystallography*; Kynoch: Birmingham, England, 1974; Vol. IV, Table 2.2.4.

(42) Cromer, D. T. *International Tables for X-ray Crystallography*; Kynoch: Birmingham, England, 1974; Vol. IV, Table 2.3.1.

Table II. Positional Parameters and Their Estimated Standard Deviations for Core Atoms in $[AuRu(H)_2(dppm)_2(PPh_3)]PF_6 \cdot CH_2Cl_2$ ($3 \cdot CH_2Cl_2$)[a]

atom	x	y	z	B, Å²
Au	0.32850 (2)	0.13458 (2)	0.07233 (1)	2.062 (6)
Ru	0.38579 (3)	−0.01017 (4)	0.14166 (3)	1.43 (1)
H1	0.417 (3)	0.056 (5)	0.097 (3)	1 (1)*
H2	0.305 (3)	0.044 (5)	0.122 (3)	1 (1)*
P1	0.2701 (1)	0.2584 (2)	0.02350 (9)	2.30 (5)
P2	0.5078 (1)	−0.0645 (1)	0.19648 (8)	1.55 (4)
P3	0.4390 (1)	0.0612 (2)	0.23656 (8)	1.63 (4)
P4	0.3232 (1)	−0.1246 (1)	0.16661 (8)	1.63 (4)
P5	0.3381 (1)	−0.1062 (1)	0.05982 (8)	1.74 (4)
C23	0.5143 (4)	−0.0212 (5)	0.2718 (3)	1.6 (2)
C45	0.3184 (5)	−0.1964 (6)	0.1029 (3)	2.4 (2)

[a] Starred values are for atoms refined isotropically. Counterion, solvent molecule, and phenyl group positional parameters are provided in the supplementary material. Anisotropically refined atoms are given in the form of the isotropic equivalent thermal parameter defined as $^4/_3[a^2\beta_{11} + b^2\beta_{22} + c^2\beta_{33} + ab(\cos\gamma)\beta_{12} + ac(\cos\beta)\beta_{13} + bc(\cos\alpha)\beta_{23}]$.

Table III. Positional Parameters and Their Estimated Standard Deviations for Core Atoms in $[Ir(H)_2(bpy)(PPh_3)_2]PF_6 \cdot CH_2Cl_2$ ($4 \cdot CH_2Cl_2$)[a]

atom	x	y	z	B, Å²
Ir	0.13524 (2)	0.20961 (1)	0.05962 (1)	1.546 (3)
P1	0.3300 (1)	0.21950 (6)	0.07623 (8)	1.52 (3)
P2	−0.0538 (1)	0.23092 (7)	0.02923 (9)	1.78 (3)
H1	0.158 (5)	0.227 (2)	−0.022 (3)	1 (1)*
H2	0.138 (6)	0.277 (3)	0.081 (4)	3 (2)*
N	0.1304 (4)	0.1102 (2)	0.0484 (3)	1.76 (9)
C2	0.1239 (5)	0.0787 (3)	0.1151 (3)	1.9 (1)
C3	0.1313 (6)	0.0152 (3)	0.1164 (4)	2.8 (1)
C4	0.1445 (6)	−0.0168 (3)	0.0509 (4)	3.0 (1)
C5	0.1501 (5)	0.0143 (3)	−0.0162 (4)	2.2 (1)
C6	0.1427 (5)	0.0780 (3)	−0.0159 (3)	2.0 (1)
N′	0.1141 (4)	0.1788 (2)	0.1725 (3)	2.0 (1)
C2′	0.1113 (5)	0.1162 (3)	0.1834 (3)	2.1 (1)
C3′	0.1000 (6)	0.0925 (3)	0.2550 (4)	2.9 (1)
C4′	0.0926 (6)	0.1306 (4)	0.3158 (4)	3.5 (1)
C5′	0.0962 (7)	0.1935 (3)	0.3046 (4)	3.4 (2)
C6′	0.1061 (6)	0.2157 (3)	0.2329 (4)	2.7 (1)

[a] See footnote *a* of Table II.

anion in each case. The final positional and thermal parameters of the refined atoms within the coordination cores are given in Tables II and III. ORTEP drawings of the cations including the labeling schemes and selected distances and angles are shown in Figures 1 and 4. Complete listings of thermal parameters, positional parameters, calculated positions for the hydrogen atoms, distances, angles, least-squares planes, and structure factor amplitudes are included as supplementary material.[43]

Results and Discussion

$[AuRu(H)_2(dppm)_2(PPh_3)]PF_6$ (3). The addition of 1 equiv of $AuPPh_3NO_3$ to $Ru(H)_2(dppm)_2$ in an acetone solution gave the cationic gold–ruthenium dihydride compound as the nitrate salt. This product was then metathesized with KPF_6 to give **3** in good yield. A single-crystal X-ray diffraction analysis of this compound was carried out in order to determine the nature of the ruthenium–gold interaction and the bonding mode of the two hydride ligands. These questions could not be answered from the solution NMR and IR data alone (vide infra).

The structure of the coordination core of **3** with selected distances and angles is shown in Figure 1. The structure consists of a $Au(PPh_3)$ unit bonded to a bischelated $Ru(dppm)_2$ moiety, with an approximately planar $Ru(H)_2AuP$ arrangement and a nearly linear P3–Ru–P5 (168.46 (7)°) grouping perpendicular to this plane. The hydrides bridge the Ru–Au bond such that they are approximately trans to phosphorus atoms of the dppm chelates (H1–Ru–P4 = 159 (2)°; H2–Ru–P2 = 163 (2)°). The Au–P1 vector is approximately trans to the Ru atom (P1–Au–Ru = 170.95 (5)°) and makes angles of 148 (2) and 134 (2)° with H1 and H2, respectively. H1 and H2 bridge asymmetrically, being somewhat closer to the Ru atom than to the Au atom (average Ru–H = 1.71 (6) Å; average Au–H = 1.98 (6) Å). The average Ru–H distance is similar to values previously observed for hydrides bridging to Ru (1.61 (4) Å in $[Au_2Ru(H)_2(dppm)_2(PPh_3)_2](NO_3)_2$ (**1**),[2] 1.62 (5) Å in $RuRh(\mu\text{-}H)(Ph)(cod)(PhPCH_2PPh_2)(dppm)$,[44] typical range 1.6–1.9 Å[45]). The average Au–H distance (1.98 (6) Å) is slightly long compared to previously determined values (1.77 (4) Å in **1** and 1.7 (1) Å in $AuCr(\mu\text{-}H)(CO)_5(PPh_3)$[28]). The Ru–Au distance (2.694 (1) Å) is shorter than values observed in other Ru–Au clusters (for example, average 2.781 (0) Å in **1**, 2.748 (1) Å in $Ru_3Au(\mu_3\text{-}S)(H)(CO)_9(PPh_3)$,[46] and 2.795 (2) Å in $Au_2Ru_4(\mu\text{-}H)(\mu_3\text{-}H)(dppm)(CO)_{12}$[22]). The short Ru–Au distance in **3** may be a result of the two hydride bridges, but this is not clear. In $AuCo(CO)_3(PPh_3)_2$[47] the Au–Co distance (2.450 (1) Å) is also short and, therefore, the short Ru–Au distance in **3** may be due to the isolated nature of the Ru–Au bond. The Ru–Au bonds in the other compounds above involve Au atoms that are bonded to two or more metal atoms. No other structurally characterized RuAu clusters have a simple $Ru\text{–}AuPPh_3$ moiety similar to that of **3**, so meaningful comparisons are not possible. The Au–P1 distance (2.252 (2) Å) and average Ru–P distances (2.331 (2) Å) compare well with those in **1** (2.283 (1) and 2.361 (1) Å, respectively) and are similar to values observed in other heterometallic clusters[3–6] and Ru–dppm-chelated compounds.[44]

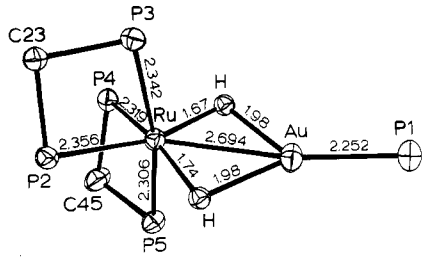

Figure 1. ORTEP drawing of the coordination core of **3** with selected bond distances. Ellipsoids are drawn with 50% probability boundaries. Phenyl rings have been omitted for clarity. Selected angles (deg) are as follows: Ru–Au–P1 = 170.95 (5); H1–Au–P1 = 148 (2); H2–Au–P1 = 134 (2); Au–Ru–P2 = 134.53 (5); Au–Ru–P3 = 97.94 (5); Au–Ru–P4 = 128.78 (5); Au–Ru–P5 = 93.34 (5); H1–Ru–H2 = 94 (3); H1–Ru–P4 = 159 (2); H1–Ru–P5 = 88 (2); H2–Ru–P2 = 163 (2); H2–Ru–P3 = 93 (2); H2–Ru–P4 = 84 (2); P2–Ru–P3 = 70.25 (6); P2–Ru–P4 = 96.69 (6). Esd's in the last significant figure for Au–Ru, M–P, and M–H distances are 1, 2, and 6, respectively.

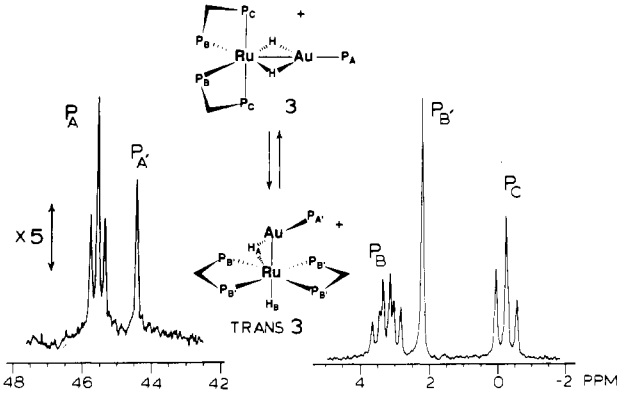

Figure 2. $^{31}P\{^1H\}$ NMR spectra of **3** and its trans isomer. Assignments are based on arguments in the text.

(43) See paragraph at end of paper regarding supplementary material.

(44) Delavaux, B.; Chaudret, B.; Dahan, F.; Poilblanc, R. *Organometallics* **1985**, *4*, 935.
(45) Teller, R. G.; Bau, R. *Struct. Bonding (Berlin)* **1981**, *44*, 1. Bau, R.; Teller, R. G.; Kirtley, S. W.; Kottzle, T. F. *Acc. Chem. Res.* **1979**, *12*, 176.
(46) Bruce, M. I.; Shawkataly, O. B.; Nicholson, B. K. *J. Organomet. Chem.* **1985**, *286*, 427.
(47) Bashkin, J.; Briant, C. E.; Mingos, D. M. P.; Wardle, R. W. M. *Transition Met. Chem. (Weinheim, Ger.)* **1985**, *10*, 113.

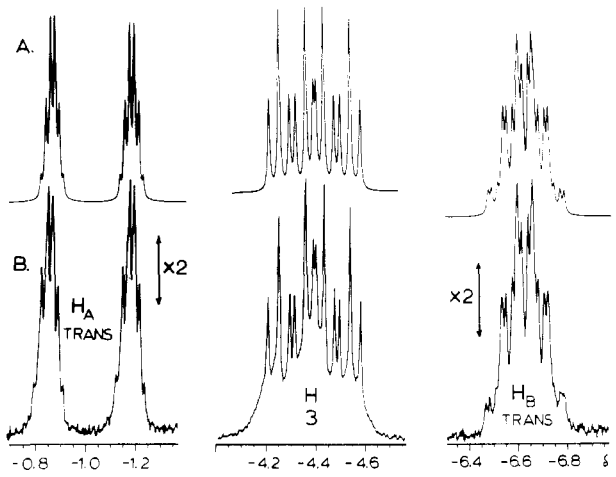

Figure 3. ^1H NMR spectra of **3** and its trans isomer (see Figure 2) in the hydride region recorded with use of acetone-d_6 as solvent at 25 °C. Parts B and A are observed and simulated traces, respectively. Coupling constants used in the simulations are given in the text, and assignments are defined in Figure 2.

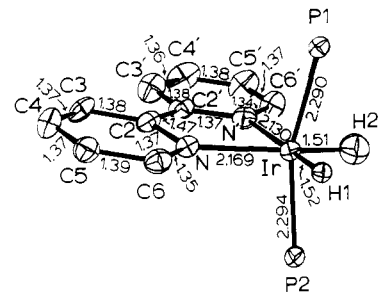

Figure 4. ORTEP drawing of the coordination core of **4**. Ellipsoids are drawn with 50% probability boundaries. Phenyl rings have been omitted for clarity. Selected angles (deg) are as follows: P1–Ir–P2 = 161.82 (5); P1–Ir–H1 = 83 (2); P1–Ir–H2 = 82 (2); P1–Ir–N = 97.3 (1); P1–Ir–N′ = 93.9 (1); P2–Ir–H1 = 86 (2); P2–Ir–H2 = 83 (2); P2–Ir–N = 99.2 (1); P2–Ir–N′ = 97.5 (1); H1–Ir–H2 = 90 (3); H1–Ir–N = 99 (2); H1–Ir–N′ = 175 (2); H2–Ir–N = 171 (2); H2–Ir–N′ = 94 (2); N–Ir–N′ = 76.7 (2); Ir–N–C2 = 114.9 (4); Ir–N–C6 = 126.2 (4); Ir–N′–C2′ = 116.6 (4); Ir–N′–C6′ = 125.0 (4). Esd's in the last significant figure for Ir–P, Ir–H, Ir–N, N–C, and C–C distances are 2, 6, 5, 1, and 1, respectively.

There is not a significant lengthening of the Ru–P bonds trans to the bridging hydrides (2.356 (2) and 2.319 (2) Å) relative to those of the mutually trans phosphorus atoms (2.342 (2) and 2.306 (2) Å). This is in agreement with observations of others that clearly show that bridging hydrides do not exhibit a large trans influence,[48] similar to what is observed in **1**.[2] If the hydrides in **3** were bonded to Ru in a terminal fashion, the Ru–P bonds trans to the hydrides would be expected to be significantly longer. This is clearly evident in *cis*-$(H)_2Ru(dppe)_2$, where the Ru–P distances trans to the hydrides average 2.312 (3) Å compared with 2.283 (3) Å for those that are mutually trans.[49]

The $^{31}P\{^1H\}$ NMR spectrum of **3** (25 °C, acetone) was consistent with its solid-state structure. A trace of the spectrum is shown in Figure 2 and consists of three multiplets of 1:2:2 integration due to the phosphorus atoms of **3**, along with two singlets of 1:4 integration, which are assigned to a trans isomer of **3** (vide infra). The triplet at δ 45.67 (P_A in Figure 2) is due to the gold phosphine phosphorus which is coupled to two equivalent P_B atoms. The coupling to P_C is expected to be small and unobservable by comparison to the ^{31}P spectrum of **1**.[2] Compound **3** was also synthesized with PMe_2Ph in place of PPh_3 on the Au.[50] In this case the only resonance to shift significantly was P_A, δ 19.34 in $[AuRu(H)_2(dppm)_2(PMe_2Ph)]PF_6$. Therefore, P_B and P_C are assigned as dppm phosphorus atoms and P_A as the PPh_3. The P_C atoms (δ –0.26) couple to the two equivalent P_B atoms, resulting in a triplet (J = 36.9 Hz). The P_B atoms (δ 3.72) couple to the two equivalent P_C atoms and to the P_A atom, resulting in the triplet of doublets (J = 36.9 Hz, J = 23.8 Hz). A selectively phosphorus decoupled ^1H NMR experiment (vide infra) and a successful $^{31}P\{^1H\}$ NMR simulation confirmed this AB_2C_2 assignment.

The ^1H NMR spectrum of **3** (25 °C, acetone-d_6) was recorded in the hydride region and is shown in Figure 3. The spectrum with selective phosphorus decoupling is included as supplementary material.[43] The multiplet resonance is centered at δ –4.4, with two multiplets due to a trans isomer of **3** (vide infra). The selective P-decoupling results supported the above assignment of P_A, P_B, and P_C and yielded all of the P–H coupling constants (see Experimental Section and Figure 3). The multiplet was successfully simulated and is shown in Figure 3. This assignment was further confirmed by comparison to the spectrum of the analogous $[RuCu(H)_2(dppm)_2PCy_3]BF_4$ complex.[51] An important result of this NMR analysis was the determination of the $J_{(\mu\text{-H})\text{-}P_A}$ coupling constant in the $(\mu\text{-}H)AuPPh_3$ unit to be 54.0 Hz. This is smaller than the values of 105 Hz in $[AuCr(\mu\text{-H})(CO)_5(PPh_3)]$[28] and 79.4 Hz in $[(H_2)(PPh_3)_3Ir(\mu\text{-H})AuPPh_3]BF_4$,[52] both of which resulted from a transoid PPh_3–Au–H arrangement, and that of 74.8 Hz in **1**.[2] The magnitude of the $(\mu\text{-}H)AuPPh_3$ coupling constant suggests that, in solution, P1 is not simply trans to the Ru–Au bond but is in rapid equilibrium between trans and cis (μ-H)–Au–P stereochemistries, giving an average and thus a larger coupling constant than would be expected due to the stereochemistry seen in the solid-state structure of **3**. A value of 31 Hz was observed for compound **2**, which is thought to have an analogous $Ir(\mu\text{-}H)_2AuP$ dynamic stereochemistry.[2]

Although **3** was the only compound crystallized from a CH_2Cl_2–Et_2O solution, it was not the only species present in solution. There was NMR evidence for an isomer of **3** (see Figures 2 and 3) that has the hydride ligands arranged in a trans stereochemistry rather than cis, as in the solid-state structure of **3**. This can be seen by observing the –70 °C $^{31}P\{^1H\}$ NMR spectrum of **3**. When crystals of **3** were dissolved at –70 °C in CH_2Cl_2 solution, only signals due to **3** were present (vide supra), but when this solution was allowed to warm to room temperature, peaks due to the trans isomer of **3** appeared (Figures 2 and 3; $^{31}P\{^1H\}$ NMR δ 44.61 (s, int = 1), 2.18 (s, int = 4); ^1H NMR δ –1.0 (d of sextets, $J_{H_A\text{-}H_{A'}}$ = 98.1 Hz, $J_{H_A\text{-}P_{B'}}$ = 5.8 Hz, $J_{H_A\text{-}H_B}$ = 4.7 Hz), –6.6 (mult, $J_{H_B\text{-}P_{A'}}$ = 12.2 Hz, $J_{H_B\text{-}P_{B'}}$ = 19.4 Hz, $J_{H_B\text{-}H_A}$ = 4.7 Hz). These coupling constants were obtained from the ^1H NMR spectrum with selective phosphorus decoupling (supplementary material). Successful simulation of the multiplet resonances was achieved by using these coupling constants and is shown in Figure 3. The proposed structure of the trans isomer is shown in Figure 2 and is consistent with the NMR data. This cis–trans isomerization is not surprising in that the ruthenium dihydride starting material, $Ru(H)_2(dppm)_2$, exists as cis and trans isomers (4:1 ratio), which interconvert via a rapid temperature-independent equilibrium.[38] Further studies of this trans isomer are under current investigation.

$[Ir(H)_2(bpy)(PPh_3)_2]X$ (X = BF_4, PF_6 (4)). Previous work with $[AuIr(H)_2(bpy)(PPh_3)_3](BF_4)_2$ (**2**), which included a single-crystal X-ray analysis, resulted in indirect evidence that supported a bridging dihydride arrangement.[2] Comparison of these structural data with similar data for $[Ir(H)_2(bpy)(PPh_3)_2]PF_6$ (**4**) can in principle provide further support for a bridging dihydride formulation. The reaction of excess bipyridine with $[Ir(H)_2(PPh_3)_2((CH_3)_2CO)_2]BF_4$ with the use of acetone as solvent followed by metathesis with NH_4PF_6 resulted in the formation

(48) Immirzi, A.; Porzio, W.; Bachechi, F.; Zambonelli, L.; Venanzi, L. M. *Gazz. Chim. Ital.* **1983**, *113*, 537.
(49) Pertici, P.; Vitulli, G.; Porzio, W.; Zocchi, M. *Inorg. Chim. Acta* **1979**, *37*, L521.
(50) This compound was synthesized in a way analogous to that of **3** except with the use of $Au(PMe_2Ph)NO_3$ in place of $AuPPh_3NO_3$. PMe_2Ph was synthesized according to: Frajerman, C.; Meunier, B. *Inorg. Synth.* **1983**, *22*, 133.
(51) Delavaux, B.; Arliguie, T.; Chaudret, B.; Poilblanc, R. *Nouv. J. Chim.* **1986**, *10*, 619.
(52) Lehner, H.; Matt, D.; Pregosin, P. S.; Venanzi, L. M. *J. Am. Chem. Soc.* **1982**, *104*, 6825.

of **4** in high yield.[2] Spectroscopic data, including $^{31}P\{^1H\}$ and ^1H NMR, IR, and conductivity measurements, are consistent with this formulation. The structure was determined at −85 °C by X-ray diffraction and consisted of well-separated cations, PF_6^- anions, and a CH_2Cl_2 solvent molecule. The structure of the cation of **4** with selected distances and angles is shown in Figure 4. In this determination the hydride ligands were located and refined.

The structure of the cation of **4** consists of a planar $(N)_2IrH_2$ arrangement with a slightly bent P1–Ir–P2 (161.82 (5)°) grouping perpendicular to this plane. The bending of the P1–Ir–P2 group is such that the phosphine groups are displaced away from the bpy ligand toward the hydride ligands. Thus, the average P–Ir–N and P–Ir–H angles are 97.0 (1) and 83 (2)°, respectively. The P1–Ir–P2 angle in **4** is somewhat smaller than in $[Ir(H)_2(PPh_3)_2((CH_3)_2CO)_2]BF_4$[53] (171.63 (8)°) and **2** (171.72 (9)°). The halves of the bpy ligand are each planar within experimental error, and the dihedral angle between these planes is only 4.3°. Distances and angles within the bpy ligand are normal.[54,55] The nitrogen atoms are very nearly trans to the hydride ligands (average H–Ir–N trans angle 173 (2)°). The Ir–N distances (average 2.150 (5) Å) are longer than those observed in **2** (2.102 (8) Å) and in $[Ir(bpy)_3](ClO_4)_3$ (average 2.04 (1) Å),[54] as well as the Ir–N bond trans to the N-bonded bpy in $[Ir(bpy)\text{-}C,N)(bpy\text{-}N,N')_2](ClO_4)_3$ (2.053 (5) Å), but similar to the Ir–N distance that is trans to the C-bonded bpy in this same complex (2.135(5) Å).[55] Since a terminal hydride and a C-bonded bpy are strong structural trans-influence ligands, they would be expected to cause a similar lengthening of the trans Ir–N bond relative to that of weaker trans-influence ligands, including bridging hydrides.[4-8] The shorter Ir–N bond distances in **2** compared with those in **4** are not due to a difference in coordination number since **4** is six-coordinate while **2** is formally seven-coordinate, and **2** is certainly more sterically crowded due to the presence of the Ir–Au bond. In fact, this trend is observed in the Ir–P distances, as these bond lengths increase upon going from **4** (average 2.292 (2) Å) to **2** (average 2.351 (2) Å). Thus, the shorter Ir–N bond lengths in **2** are due to the weak structural trans influence of the bridging hydrides compared with the stronger influence of terminal hydrides in **4**, further supporting the bridging dihydride formulation in **2** as previously proposed. This has been further verified by a calculation of the optimum hydride positions in **2** with the use of Orpen's potential energy minimization computer program.[56]

The Ir–H distances (average 1.51 (6) Å) in **4** are somewhat short compared to the established range for second-row- and third-row-metal–hydride distances (1.6–1.7 Å), though this range was based partially on data from neutron diffraction studies. Since X-ray-determined bond lengths tend to be up to 0.1 Å shorter than their neutron-determined counterparts,[57] the Ir–H distances in **4** are probably normal.

AuL and AgL Adducts of $[Ir(H)_2(bpy)(PPh_3)_2]BF_4$. Stable 1:1 adducts of $[Ir(H)_2(bpy)(PPh_3)_2]^+$ were synthesized and isolated by the reaction of the BF_4^- salt of **4** with several electrophilic fragments containing Au or Ag. The addition of cold (−78 °C) CH_3OH solutions of AgO_3SCF_3 and $AgNO_3$ to cold CH_2Cl_2 solutions of the BF_4^- salt of **4** produced respectively $[AgIr(H)_2(bpy)(PPh_3)_2](O_3SCF_3)(BF_4)$ (**5**) and $[AgIr(H)_2(bpy)(PPh_3)_2(NO_3)](BF_4)$ (**6**) in high yield. As previously reported,[2] the reaction of **4** with $AuPPh_3NO_3$ at −60 °C afforded $[AuIr(H)_2(bpy)(PPh_3)_3](BF_4)_2$ (**2**) after anion metathesis. The mixing of a CH_2Cl_2–CH_3CN solution of the BF_4^- salt of **4** with $Au(CH_3CN)_2BF_4$ in CH_3CN at 0 °C produced $[AuIr(H)_2(bpy)(PPh_3)_2(CH_3CN)](BF_4)_2$ (**7**). All of these adducts were isolated as white to cream-colored solids, which dissolved to give nearly colorless to pale yellow solutions (**4** was yellow in the solid state and bright yellow in solution). Complexes **2**, **5**, and **6** were stable in both the solid and solution state at 25 °C, in contrast to the analogous compounds $[AuIr(H)_2(PPh_3)_3((CH_3)_2CO)_2]^{2+}$ and $[AuIr(H)_2(PPh_3)_3(NO_3)]^+$, which decomposed into both homo- and heterometallic complexes above −20 °C.[5,58] Complex **7** was unstable at room temperature and in the presence of water and gradually decomposed to produce a dark material. Reactivity and spectroscopic studies of **7** were therefore performed on freshly filtered and reprecipitated samples.

The formation of 1:1 adducts of $[Ir(H)_2(bpy)(PPh_3)_2]^+$ was the only observed reaction. Unlike $[Ir(H)_2(PPh_3)_2((CH_3)_2CO)]^+$, which reacted sequentially with 1–3 equiv of $AuPPh_3NO_3$ to form $[AuIr(H)_2(PPh_3)_3(NO_3)]^+$, $[Au_2Ir(H)(PPh_3)_4NO_3]^+$, and $[Au_3Ir(PPh_3)_5NO_3]^+$,[5,58] the adducts of $[Ir(H)_2(bpy)(PPh_3)_2]^+$ showed no reaction with additional equivalents of AuL^+ (L = PPh_3, CH_3CN) or AgL (L = NO_3, O_3SCF_3). However, using less than 1 equiv of the group 1B metal did not give Ir_2M adducts as in the cases of $\{[fac\text{-}IrH_3(PMe_2Ph)_3]_2Ag\}^+$[29] and $\{[ReH_7\{P(i\text{-}Pr)_2Ph\}_2]_2Ag\}^+$.[21] This was somewhat surprising in that complexes **5** and **6** have a very labile triflate or nitrate anion associated with the silver atom and might afford open coordination sites on the silver for a second molecule of $[Ir(H)_2(bpy)(PPh_3)_2]^+$. Yet solutions containing 0.5 equiv of AgO_3SCF_3 with **4** showed a 50:50 mixture of **4** and **5**, while solutions containing 1 or 2 equiv of AgO_3SCF_3 with **4** showed only **5**, as determined by $^{31}P\{^1H\}$ NMR at −80 °C. Thus, only 1:1 adducts were formed.

The characterization data for complexes **5**–**7** compared well with those for **2** and was consistent with the formation of 1:1 adducts in which the Ir–M bond (M = Au, Ag) is bridged by both hydride ligands as shown:

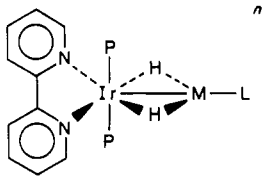

5 (M = Ag, L = solvent, n = +2), **6** (M = Ag, L = NO_3, n = +1), **7** (M = Au, L = CH_3CN, n = +2), **8** (M = Ag, L = PPh_3, n = +2)

The silver complexes **5** and **6** showed evidence of a dissociative equilibrium of the type

$$[AgIr(H)_2(bpy)(PPh_3)_2]^{2+} \rightleftharpoons Ag^+ + [Ir(H)_2(bpy)(PPh_3)_2]^+ \quad (1)$$

Evidence for eq 1 was obtained by $^{31}P\{^1H\}$ NMR for the silver complexes **5** and **6**. When 1 equiv of the starting material **4** was added to **5** and dissolved in CH_2Cl_2 at 25 °C, extremely broad peaks were observed in the vicinity where peaks due to **4** and **5** should occur. When the temperature was lowered to −15 °C, the peaks began to sharpen, due to the slowing of the rate of the reaction shown in eq 1. Identical behavior was observed with **6**. The IrAu complexes **2** and **7** did not show dynamic behavior. When **4** (or $AuPPh_3NO_3$) was added to **2**, $^{31}P\{^1H\}$ NMR spectra taken at 25 °C with use of CH_2Cl_2 as solvent showed only sharp signals due to **2** and **4** (or $AuPPh_3NO_3$). Similarly, spectra of **7** did not exhibit peak broadening or shifting at room temperature when **4** was added to a CH_2Cl_2 solution of **7**.

The $^{31}P\{^1H\}$ NMR spectra of compounds **5**–**7** all showed upfield shifts from the starting material **4** for the iridium phosphine signal. The $^{31}P\{^1H\}$ NMR spectra of complexes **4**–**7** were recorded at −15 °C. At this temperature **4** appeared at δ 18.2. CH_2Cl_2 solutions of **5**–**7** gave rise to singlets at δ 5.1, 5.9, and 2.3, respectively. Note that complex **5** showed a concentration-dependent ^{31}P NMR shift (see Experimental Section). Lowering the temperature to −80 °C produced slight changes in the chemical shifts, as is usual, and showed only signals due to the adducts **5**–**7**. The absence of signals due to **4** indicated that the equilibrium shown in eq 1 lies to the left; however, $^{Ag}Ir^{P}Ph_3$ couplings were not observed for any of the compounds under all conditions applied.

(53) Crabtree, R. H.; Hlatky, G. G.; Parnell, C. P.; Segmüller, B. E.; Uriarte, R. J. *Inorg. Chem.* **1984**, *23*, 354.
(54) Hazell, A. C. *Abstracts*; 18th Danish Crystallography Meeting, Risø, Denmark; Wiley: New York, 1982; paper 24.
(55) Nord, G.; Hazell, A. C.; Hazell, R. G.; Farver, O. *Inorg. Chem.* **1983**, *22*, 3429.
(56) Orpen, A. G. *J. Chem. Soc., Dalton Trans.* **1980**, 2509.
(57) Hlatky, G. G.; Crabtree, R. H. *Coord. Chem. Rev.* **1985**, *65*, 1.
(58) Casalnuovo, A. L. Ph.D. Thesis, University of Minnesota, 1984.

^{1}H NMR spectra were consistent with fast dynamic behavior for the IrAg complexes **5** and **6** and slow or no exchange for the IrAu complexes **2** and **7**. The hydride region of the ^{1}H NMR spectrum of **4** at 25 °C with use of $CDCl_3$ as solvent showed a triplet at δ −19.4 due to coupling between the iridium hydrides and the two equivalent iridium phosphine phosphorus atoms (J = 16.7 Hz).[2] Couplings of this magnitude were also observed for $[Ir(H)_2(PPh_3)_2((CH_3)_2CO)_2]^+$ (J = 15.8 Hz) and $Ir(H)_2(PPh_3)_2NO_3$ (J = 16 Hz) under similar conditions.[5,58] The AgO_3SCF_3 adduct of **4**, complex **5**, gave a sharp triplet hydride signal at δ −16.9 with J_{P-H} = 12.8 Hz at −15 °C with use of CD_2Cl_2 as solvent. When the system was cooled to −70 °C, the hydride resonance appeared as a broad singlet. These results are consistent with fast intermolecular exchange of AgO_3SCF_3 groups at −15 °C and an intermediate exchange rate at lower temperature. In the fast-exchange region the signal should correspond to an average of the signals due to the species in eq 1, weighted by their relative concentrations. From ^{31}P NMR studies, it was established that the equilibrium lies to the left. Thus the hydride chemical shifts and P–H coupling constants are representative of the IrAg adduct.

The $AgNO_3$ adduct of **4**, complex **6**, behaved similarly. At 20 °C with use of CD_2Cl_2 as solvent, the hydride signal appeared as a sharp triplet at δ −17.3 (J_{P-H} = 13.4 Hz). When the temperature was lowered to −15 °C, the signal broadened and finally became a broad doublet (J = 59 Hz) at −80 °C. The doublet splitting is assigned to Ag–H coupling, though separate ^{109}Ag and ^{107}Ag couplings were not resolved. A coupling of comparable magnitude was observed for $[(fac\text{-}IrH_3P_3)_2Ag]^+$ (49.5 Hz), though separate ^{109}Ag and ^{107}Ag couples were not resolved in this case either.[29] The effect of the lability of Ag on the hydride spectra of heterometallic complexes containing Ag has been observed and discussed previously.[21,29]

The IrAu complexes did not show any dynamic NMR behavior. Compound **2** gave rise to a doublet of triplets in the hydride region of the ^{1}H NMR spectrum (δ −13.3, J_{IrP-H} = 11 Hz, J_{AuP-H} = 31 Hz) at 25 °C.[2] The observation of HAuPPh$_3$ coupling indicates that dissociation of the $AuPPh_3$ fragment from **4** cannot be occurring quickly on the ^{1}H NMR time scale at this temperature. The magnitude of the HIrPPh$_3$ and HAuPPh$_3$ couplings in **2** is very similar to those in $[AuIr(H)_2(PPh_3)_3((CH_3)_2CO)_2]^{2+}$ (J = 10 and 26 Hz, respectively) and $[AuIr(H)_2(PPh_3)_3NO_3]^+$ (J = 11 and 30 Hz, respectively).[5,58] The $Au(CH_3CN)^+$ adduct of **4**, complex **7**, also showed no evidence of dynamic NMR behavior. ^{1}H NMR spectra of **7** at −15 °C with CD_2Cl_2 as solvent showed a triplet hydride resonance at δ −15.6 (J = 10.4 Hz) that did not change upon lowering the temperature to −70 °C.

Several trends become apparent from examination of the ^{1}H NMR data of compounds **5**–**7**. First, the magnitude of the HIrPPh$_3$ coupling constant decreased by 3–6 Hz upon coordination of the group 1B fragment to **4**. This same trend was observed in complexes where NO_3^- or two acetone ligands were bonded to Ir in place of bpy trans to the hydrides.[5,58] The Ir–H bond should weaken upon going from a terminal- to a bridge-bonding mode, which would cause a reduction of the HIrPPh$_3$ coupling constant. This was observed in **2**, which was structurally characterized and shown to contain an Ir–Au bond that is most likely bridged by both hydrides (vide supra). Thus, the reduction in the P–H coupling constants in **5**–**7** support this bridging dihydride formulation for these complexes as well. Second, the coordination of the group 1B fragment to **4** generally resulted in downfield shifts for the hydride signal. This trend was also observed in the complexes where NO_3^- or acetone was coordinated to Ir.[5,58] The magnitude of the downfield shifts ranged from 2 to 10 ppm. Third, the Ag adducts of **4** were all dissociatively labile, whereas the Au complexes were not. This trend is followed in the complexes where bpy has been formally replaced by NO_3^-, but spin-saturation-transfer experiments have shown that $[AuIr(H)_2(PPh_3)_3((CH_3)_2CO)_2]^{2+}$ is in slow equilibrium with $AuPPh_3^+$ and $[Ir(H)_2(PPh_3)_2((CH_3)_2CO)_2]^+$.[5,58]

Infrared spectra of complexes **5**–**7** were measured in the solid state in an attempt to confirm the bridging nature of the hydrides. Peaks were not observed in the terminal hydride region (1800–2300 cm^{-1}) of the spectra. This is typical of IrAu hydride compounds in general, which are thought to have the Ir(μ-H)Au arrangement and as such are not expected to show peaks in this spectral region. The bridging hydride region, however, was obscured by other ligand absorptions, so bridging hydride vibrations were not observed. Infrared spectroscopy was useful in detecting coordinated acetonitrile in **7** (ν(CN) = 2331, 2304 cm^{-1}). Peaks for coordinated acetonitrile are generally weak, occur in pairs, and usually occur at higher energy than those of the free ligand (2287, 2251 cm^{-1}).[59] IR measurements also established that in the solid state the NO_3^- group in **6** was bound to the silver ($\nu(NO_3$ bound) = 1490, 1480, 1268 cm^{-1}) and that the CF_3SO_3 group in **5** was not bound ($\nu(CF_3SO_3$ ionic) = 1280 cm^{-1} (s, br)). This band shifts to higher wavenumber, appearing near 1380 cm^{-1} in complexes with the triflate bound to the metal in a monodentate fashion.[60]

In order to further investigate the coordination of the anions in **5** and **6**, conductance measurements were carried out. Complex **7** was too unstable in dilute solution to be studied. Measurements were taken in 3 × 10^{-4} M CH_3NO_2 solutions at 25 °C. Compounds used as standards were $[Ir(H)_2(bpy)(PPh_3)_2]BF_4$ (BF_4^- salt of **4**), a 1:1 electrolyte, and $[AuIr(H)_2(bpy)(PPh_3)_3](BF_4)_2$ (**2**), a 1:2 electrolyte. Conductance values for these compounds were 56.4 and 124 cm^2 mho mol^{-1}, respectively. The value obtained for **5** was 105 cm^2 mho mol^{-1}, which is nearer the value for the 1:2 electrolyte. Compound **6** gave a conductance of 72.3 cm^2 mho mol^{-1}, which is significantly lower than that of **5** and nearer the value for the 1:1 electrolyte. The conductivity results are consistent with the conclusions drawn from the infrared experiments. The difference in anion coordination between **5** and **6** is probably due to the better coordinating ability of the NO_3^- versus that of the $O_3SCF_3^-$ anion.

The iridium–silver complex **5** reacted with 1 equiv of PPh_3 in CH_2Cl_2 solution to produce $[Ir(H)_2(bpy)(PPh_3)_2AgPPh_3](BF_4)(O_3SCF_3)$ (**8**) in good yield. Complex **6** also formed the same phosphine dication. The ^{1}H NMR spectrum of **8** showed a broad singlet in $CDCl_3$ at 25 °C, a broad doublet of doublets (J = 51.5, 12.6 Hz) at −20 °C in CD_2Cl_2, and a doublet of quartets of doublets at δ −16.3 with apparent couplings of 51.5, 12.6, and 3.1 Hz at −80 °C in CD_2Cl_2. Selective decoupling of the phosphines was difficult due to the large size of the Ag–P coupling constant (vide infra), but it was established that the HAgPPh$_3$ coupling constant was about 10–15 Hz and that the average Ag–H coupling equaled 51.5 Hz. The hydride spectrum was successfully simulated by adding the spectrum generated with the couples $J_{^{109}Ag-H}$ = 55 Hz, J_{IrP-H} = 12.5 Hz, and J_{AgP-H} = 10.5 Hz to the spectrum generated with $J_{^{107}Ag-H}$ = 48 Hz and the 10.5- and 12.5-Hz P–H coupling constants. The ratio of Ag–H coupling constants ($J_{^{109}Ag-H}$:$J_{^{107}Ag-H}$) was 1.146, in good agreement with the ratio of the ^{109}Ag to ^{107}Ag gyromagnetic ratios (1.149), as is appropriate in complexes where couplings to silver are present.[61]

The ^{31}P{^{1}H} NMR spectrum of **8** showed a singlet at δ 3.7 of intensity 2 and two doublets centered at δ 18.0 with intensity 1 in CH_2Cl_2 at −80 °C. Spectra taken at 25 °C showed the same pattern, though the signal to noise ratio was lower. The two doublets were due to resolution of both ^{109}Ag and ^{107}Ag couplings to the PPh_3 on the silver, while no AgIrPPh$_3$ coupling was observed. The magnitude of the AgPPh_3 coupling ($J_{^{109}Ag-P}$ = 708 Hz, $J_{^{107}Ag-P}$ = 613 Hz) suggests that the Ag is indeed bound to more than one ligand, since the magnitude of the coupling decreases with increasing coordination number about Ag. This is clearly shown in the trend of $J_{^{107}Ag-P}$ (702 Hz for $AgPPh_3^+$, 496 Hz for $Ag(PPh_3)_2^+$, and 321 Hz for $Ag(PPh_3)_3^+$).[61] In the case of $PPh_3Ag(\mu_3\text{-}H)_3Ru_4(CO)_{12}$, in which the Ag is thought to cap a Ru_4 tetrahedron with three hydrides triply bridging the Ag–Ru

(59) Rhodes, M. W. Ph.D. Thesis, University of Minnesota, 1984. Thomas, R. R.; Chebolu, V.; Sen, A. *J. Am. Chem. Soc.* **1986**, *108*, 4096.
(60) Lawrance, G. A. *Chem. Rev.* **1986**, *86*, 17. Brown, S. D.; Gard, G. L. *Inorg. Chem.* **1975**, *14*, 2273. Dixon, N. E.; Jackson, W. G.; Lawrance, G. A.; Lancaster, M. J.; Sargeson, A. M. *Inorg. Chem.* **1981**, *20*, 470.
(61) Muetterties, E. L.; Alegranti, C. W. *J. Am. Chem. Soc.* **1972**, *94*, 6386.

bonds, $J_{^{107}Ag-P}$ = 601 Hz.[62] Addition of **4** to a solution of **8** produced broadened spectra at room temperature, suggesting that exchange of $AgPPh_3^+$ between $[Ir(H)_2(bpy)(PPh_3)_2]^+$ groups was occurring. Furthermore, addition of **5** to solutions of **8** also produced broadened spectra, which suggested that exchange of PPh_3 between $[AgIr(H)_2(bpy)(PPh_3)_2]^{2+}$ groups occurred as well. Infrared and conductivity data for **8** were consistent with the formulation of a 1:2 electrolyte.

Complex **8** reacted further with PPh_3 to produce homometallic Ir and Ag fragments. When a slight excess of PPh_3 was added to **8** and dissolved in CH_2Cl_2, the $^{31}P\{^1H\}$ NMR spectrum showed a singlet at δ 18.7 and two doublets centered at δ 8.3 (J = 367, 318 Hz). This is consistent with the formation of $[Ir(H)_2(bpy)(PPh_3)_2]^+$ (**4**) and $Ag(PPh_3)_3^+$.[61] Nucleophilic attack of PPh_3 on M–$AuPPh_3$ or M–$AgPPh_3$ to produce M and $M'(PPh_3)_x^+$ is a common reaction.[2,63]

Summary. Several new heterobimetallic hydrides containing Au or Ag have been synthesized. $[AuRu(H)_2(dppm)_2(PPh_3)]PF_6$ (**3**) was characterized by ^{31}P and ^1H NMR spectroscopy and single-crystal X-ray crystallography. The hydride positions were located, refined, and determined to be bridging the Ru–Au bond. ^{31}P and ^1H NMR spectroscopy provided further support for this bridging dihydride formulation due to large spin–spin coupling between the hydride ligands and the gold phosphine phosphorus atom. The bridging dihydride formulation for the previously characterized $[AuIr(H)_2(bpy)(PPh_3)_3](BF_4)_2$ (**2**)[2] was further substantiated by comparing the Ir–N bond lengths in **2** to those in $[Ir(H)_2(bpy)(PPh_3)_2]PF_6$ (**4**). The average Ir–N bond length in **2** is significantly shorter than in **4**. It was argued that this is due to the weaker structural trans influence of bridging hydrides in **2** compared with the stronger influence of the terminal hydrides in **4**.

Stable 1:1 adducts of the BF_4^- salt of **4** were synthesized, including $[AgIr(H)_2(bpy)(PPh_3)_2](O_3SCF_3)(BF_4)$ (**5**), $[AgIr(H)_2(bpy)(PPh_3)_2(NO_3)](BF_4)$ (**6**), $[AuIr(H)_2(bpy)(PPh_3)_2(CH_3CN)](BF_4)_2$ (**7**), and $[AgIr(H)_2(bpy)(PPh_3)_3](O_3SCF_3)(BF_4)$ (**8**). Complexes **5–7** are interesting in that they contain labile ligands bound to the coinage metal. The ability of the group 1B metal to provide open coordination sites near a transition-metal hydride may find use in homogeneous catalysis, since evidence for catalyst improvement upon incorporation of a group 1B metal into a transition-metal cluster has been reported.[33] Complexes **5–8** were characterized by IR and ^{31}P and ^1H NMR spectroscopy and determined to have the bridging dihydride formulation in the solid state analogous to the case for **2** and **3**. In solution, however, the IrAg complexes were shown to be kinetically labile while the IrAu complexes were not. It was also found that only 1:1 adducts were formed and the hydrides were not replaced by Au or Ag. This may be due to the presence of the bpy ligand since Au_2Ir complex formation and H^+ loss occurred when the ligand trans to the hydride was a nitrate,[5] a stronger trans-effect ligand. Also, in the case of Ag, Ag–Ag bonds are not nearly as common as Au–Au bonds, and evidence suggests that Ag is more likely to bind to hydrides rather than replace them. Steric hindrance may also be a contributing factor due to the large size of the bpy and PPh_3 ligands.

Acknowledgment. This work has been supported by the National Science Foundation (Grant CHE-851923) and by the donors of the Petroleum Research Fund, administered by the American Chemical Society. We also thank the Johnson Matthey Co. for generous loans of salts of gold and iridium. B.D.A. thanks General Electric for an industrial fellowship.

Supplementary Material Available: ORTEP drawings of **3** and **4**, the ^1H NMR spectrum of the hydride resonances of **3** with selective ^{31}P decoupling, and listings of general temperature factor expressions, final positional and thermal parameters for all atoms including counterions, solvate molecules, and calculated hydrogen atom positions, least-squares planes, and distances and angles of **3** and **4** (35 pages); listings of observed and calculated structure factor amplitudes of **3** and **4** (58 pages). Ordering information is given on any current masthead page.

(62) Salter, I. D.; Stone, F. G. A. *J. Organomet. Chem.* **1984**, *260*, C71.
(63) Alexander, B. D.; Boyle, P. D.; Johnson, B. J.; Casalnuovo, J. A.; Johnson, S. M.; Mueting, A. M.; Pignolet, L. H. *Inorg. Chem.* **1987**, *26*, 2547.
(64) The periodic group notation in parentheses is in accord with recent actions by IUPAC and ACS nomenclature committees. A and B notation is eliminated because of wide confusion. Groups IA and IIA become groups 1 and 2. The d-transition elements comprise groups 3 through 12, and the p-block elements comprise groups 13 through 18. (Note that the former Roman number designation is preserved in the last digit of the numbering: e.g., III → 3 and 13.)

Contribution from the School of Chemistry, University of New South Wales, Kensington, NSW 2033, Australia

Magnetic, Spectroscopic, and Structural Characterization of Singlet ⇌ Quintet Transitions in Iron(II) Complexes of Methyl-Substituted Pyridinylthiazoles

Anthony T. Baker,[1] Harold A. Goodwin,* and A. David Rae*

Received February 24, 1987

Iron(II) and nickel(II) $[ML_3]X_2$ type complexes have been prepared where L = 2-methyl-4-(pyridin-2-yl)thiazole (2mpt), 4-methyl-2-(pyridin-2-yl)thiazole (4mpt), and 2-(6-methylpyridin-2-yl)thiazole (6mpt). Salts of both $[Fe(2mpt)_3]^{2+}$ and $[Fe(4mpt)_3]^{2+}$ have strongly temperature-dependent magnetic moments that indicate the occurrence of a singlet ($^1A_1$) ⇌ quintet ($^5T_2$) spin transition. This is confirmed by Mössbauer and electronic spectral data. $[Fe(6mpt)_3][ClO_4]_2$ is a purely high-spin species. The spin transition in $[Fe(4mpt)_3][ClO_4]_2$ is fairly abrupt and virtually complete within the range 100–300 K. The structure of this complex has been determined at 294 and 133 K. The change in temperature is accompanied by a contraction in the average Fe–N distance of 0.16 Å and a disorder–order transition in the anion orientation. Nickel complexes were prepared to allow comparisons of ligand field and structural characteristics. The structure of $[Ni(4mpt)_3][ClO_4]_2$ was determined at 294 K. Crystal data: $[Fe(4mpt)_3][ClO_4]_2$ at 294 K, space group $P\bar{3}c1$, $a = b$ = 10.223 (2) Å, c = 17.782 (6) Å, $\alpha = \beta$ = 90°, γ = 120°, Z = 2; $[Fe(4mpt)_3][ClO_4]_2$ at 133 K, space group $P\bar{3}c1$, $a = b$ = 10.145 (7) Å, c = 17.39 (1) Å, $\alpha = \beta$ = 90°, γ = 120°, Z = 2; $[Ni(4mpt)_3][ClO_4]_2$ at 294 K, space group $P\bar{3}c1$, $a = b$ = 10.246 (1) Å, c = 17.627 (3) Å, $\alpha = \beta$ = 90°, γ = 120°, Z = 2.

Introduction

Electronic spin-state transitions in iron(II) (d^6) systems can be generated in a number of ways, but one of the most effective is to modify structurally the strong-field diimine systems 2,2-bipyridine (bpy) or 1,10-phenanthroline (phen) so that the reduced field strength lies near the critical value where the quintet/singlet crossover occurs.[2] This is illustrated for example by the replacement of one pyridyl group in bpy by an imidazolyl to give 2-(pyridin-2-yl) imidazole (pyi). The spin transition in salts of

(1) CSIRO, Division of Protein Chemistry, Parkville, 3052 Victoria, Australia.
(2) Goodwin, H. A. *Coord. Chem. Rev.* **1976**, *18*, 293.

0020-1669/87/1326-3513$01.50/0 © 1987 American Chemical Society